

# Template synthesis, structure and electrochemistry of trinuclear iron(II) clathrochelate dioximates with ferrocenylboron fragments<sup>1</sup>

Yan Z. Voloshin<sup>a,\*</sup>, Tatyana E. Kron<sup>a</sup>, Vitaly K. Belsky<sup>a</sup>, Valery E. Zavodnik<sup>a</sup>,  
Yurii A. Maletin<sup>b</sup>, Sergey G. Kozachkov<sup>b</sup>

<sup>a</sup> Karpov Institute of Physical Chemistry, 103064 Moscow, Russia

<sup>b</sup> Institute of General and Inorganic Chemistry, 252142 Kiev, Ukraine

Received 13 June 1996; accepted 16 September 1996

## Abstract

Trinuclear macrobicyclic iron(II) complexes with alkyl, aryl and alicyclic dioximes have been synthesized by direct template reactions on the Fe<sup>2+</sup> ion using ferrocenylboronic acid (FcB(OH)<sub>2</sub>) as cross-linking agent. The geometry of the distorted trigonal prismatic coordination polyhedron of encapsulated iron(II) ion for each obtained compound has been determined from Mössbauer (<sup>57</sup>Fe) parameters using X-ray data for nioximate FeN<sub>x</sub><sub>3</sub>(BFC)<sub>2</sub> · 2CCl<sub>4</sub> complex (Fe–N distance 1.91 Å, bite angle 39.3°, polyhedron distortion angle 9.5°). The *fac*- and *mer*-isomers of the non-symmetrical methyl-glyoxime have been detected from the <sup>13</sup>C NMR spectrum. By electrochemical investigation, two independent redox centres were determined in molecules of synthesized complexes. © 1997 Elsevier Science S.A.

**Keywords:** Cage compounds; Ferrocenyl derivatives; X-ray diffraction; Electrochemistry

## 1. Introduction

Clathrochelate macrobicyclic ligands, completely encapsulating the metal ions, are known for a number of metal and ligand systems. The iron(II) and cobalt(III,II) clathrochelate complexes based on various dioxime molecules are formed under soft conditions with a high yield. Numerous boron-, tin- and germanium-containing iron(II) macrobicyclic complexes have been reported [1–11]. A series of these compounds was synthesized for electrochemical investigation [12,13]. The Co(III) and Co(II) clathrochelate dioximates obtained by cross-linking halogenotin- and boron-containing groups were also synthesized [14–20] and the electrochemistry of several compounds, in particular with the ferrocenylboron fragment, has been studied [18–20].

In order to study systematically the effect of peripheral substituent groups on the structure and spectra of macrobicyclic iron(II) complexes, as well as for electro-

chemical investigation, we have obtained a range of new iron(II) compounds with ferrocenylboron cross-linking group.

## 2. Experimental section

The starting materials and measurements were described in detail in previous papers [6,8,17]. Ferrocenylboronic acid was obtained by the method reported in Ref. [21]. The starting ligand designations are shown in Fig. 1.

Cyclic voltammograms were recorded in acetonitrile or dichloromethane (0.1 mol dm<sup>-3</sup> (Bu<sub>4</sub>N)BF<sub>4</sub>) using a PI-50-1 potentiostat coupled with a B7-45 tera-ohmic potentiometer as a current–voltage converter. Scan rates were varied from 5 to 50 mV s<sup>-1</sup>. A Pt microelectrode of 10 μm diameter, thoroughly polished and washed before measurements, was chosen as a working electrode. A Pt wire was applied as an auxiliary electrode. An AgCl/Ag reference electrode was connected to the cell via a salt bridge. A ferrocenium/ferrocene (Fc<sup>+</sup>/Fc) redox couple was used as an internal standard, and its potential was 475 mV in acetonitrile or

\* Corresponding author.

<sup>1</sup> To the memory of Yuri T. Struchkov with whom Y.Z.V. has enjoyed many years of very fruitful joint research.

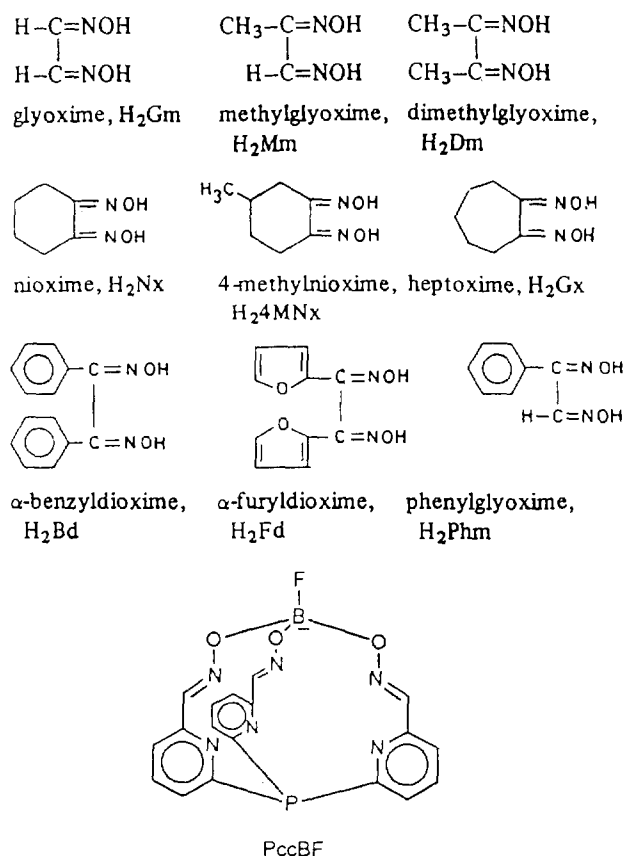


Fig. 1. The starting nitrogen-containing ligands designations.

645 mV in dichloromethane under our experimental conditions.

Solvents for electrochemical measurements were purified as recommended elsewhere, see Ref. [22] for acetonitrile and Ref. [23] for dichloromethane. The  $(\text{Bu}_4\text{N})\text{BF}_4$  salt was recrystallized from methanol–water and *iso*-propanol–water mixtures, and then dried in vacuo. All measurements were carried out under dry argon atmosphere.

### 2.1. Synthesis of clathrochelates

#### 2.1.1. $\text{FeNx}_3(\text{BFc})_2$

0.43 g of nioxime (3 mmol), 0.35 g of ferrocenylboric acid (2 mmol) and 0.20 g of  $\text{FeCl}_2 \cdot 4\text{H}_2\text{O}$  (1 mmol) were dissolved in 10 ml of methanol and stirred for 1 h. The red–orange precipitate was filtrated and washed with methanol, diethyl ether and pentane. The product was recrystallized from chloroform and dried in vacuo; yield 0.65 g (71%). Anal. Found: C, 52.3; H, 4.9; N, 9.5; Fe, 19.3.  $\text{C}_{38}\text{H}_{42}\text{N}_6\text{O}_6\text{Fe}_3\text{B}_2$  Calc.: C, 52.5; H, 4.8; N, 9.7; Fe, 19.4%.

#### 2.1.2. $\text{FeGx}_3(\text{BFc})_2$

This complex was synthesized by a similar procedure except that heptoxime (0.47 g, 3 mmol) was used instead

Table 1

Atom coordinates ( $\times 10^4$ ) and temperature factors ( $\text{\AA}^2 \times 10^3$ ) in  $\text{FeNx}_3(\text{BFc})_2 \cdot 2\text{CCl}_4$

Atom	x	y	z	U
Fe(1)	4020(2)	9198(1)	8393(1)	36(1) *
Fe(2)	2175(2)	5386(1)	10400(1)	47(1) *
Fe(3)	5694(3)	13019(2)	6424(1)	69(1) *
O(1)	1755	8553	9232	72 *
O(2)	3583	7215	8926	65 *
O(3)	3628	7891	9984	60 *
O(4)	5301	9967	6820	77 *
O(5)	5955	10306	7891	68 *
O(6)	3841	11250	7422	65 *
N(1)	2210	9333	8716	52 *
N(2)	4130	7879	8352	55 *
N(3)	4324	8527	9456	47 *
N(4)	4898	9175	7348	55 *
N(5)	5456	9623	8465	53 *
N(6)	3199	10598	7905	46 *
B(1)	2805	7612	9604	41 *
B(2)	5270	10768	7185	43 *
C(1)	1364	10200	8490	40 *
C(2)	-110	10403	8675	57 *
C(3)	-827	11526	8435	76 *
C(4)	-309	12046	7628	82 *
C(5)	1117	12004	7569	52 *
C(6)	1924	10952	7977	42 *
C(7)	4674	7610	7718	51
C(8)	4832	6631	7587	70 *
C(9a)	6093	6470	6879	67
C(9b)	5068	6798	6659	70
C(10)	5998	7227	6252	111 *
C(11)	5928	8270	6330	60 *
C(12)	5149	8363	7131	50 *
C(13)	5348	8562	9734	44 *
C(14)	5764	7981	10551	46 *
C(15)	7169	8005	10532	68 *
C(16)	7384	8972	10173	64 *
C(17)	7124	9431	9287	50 *
C(18)	5945	9237	9161	39 *
C(19)	2133	6891	10233	37 *
C(20)	880	6794	10304	46 *
C(21)	608	6113	11050	52 *
C(22)	1727	5709	11466	57 *
C(23)	2697	6169	10969	47 *
C(24)	3216	4955	9421	56 *
C(25)	2004	4872	9509	64 *
C(26)	1827	4193	10261	68 *
C(27)	2926	3842	10645	68 *
C(28)	3854	4300	10126	69 *
C(29)	5871	11535	6520	51 *
C(30)	7114	11656	6522	78 *
C(31)	7336	12386	5758	106 *
C(32)	6277	12713	5347	76 *
C(33)	5409	12182	5807	55 *
C(34)	4368	13509	7257	108 *
C(35)	5606	13429	7407	127 *
C(36)	6075	14044	6772	127 *
C(37)	5208	14508	6242	116 *
C(38)	4011	14234	6512	182 *
C(100)	126	7467	7329	102
C(101)	8160	9659	4317	76

\* Equivalent isotropic U defined as one third of the trace of the orthogonalized  $U(i,j)$  tensor.

of nioxime; yield 0.75 g (85%). Anal. Found: C, 54.0; H, 5.4; N, 9.1; Fe, 18.7.  $C_{41}H_{48}N_6O_6Fe_3B_2$  Calc.: C, 54.1; H, 5.3; N, 9.2; Fe, 18.5%.

### 2.1.3. $Fe(4MNx)_3(BFc)_2$

This complex was synthesized as previously but 4-methyl-nioxime (0.47 g, 3 mmol) was used instead of heptoxime; yield 0.55 g (60%). Anal. Found: C, 53.9; H, 5.4; N, 9.4; Fe, 18.5.  $C_{41}H_{48}N_6O_6Fe_3B_2$  Calc.: C, 54.1; H, 5.3; N, 9.2; Fe, 18.5%.

### 2.1.4. $FeDm_3(BFc)_2$

This complex was obtained in the same manner as  $FeNx_3(BFc)_2$  except that methanol was replaced by ethanol and dimethylglyoxime (0.35 g, 3 mmol) was used instead of nioxime;  $Na_2CO_3$  (1 g) was added for acid neutralization; yield 0.30 g (38%). Anal. Found: C, 48.2; H, 4.7; N, 10.7; Fe, 21.1.  $C_{32}H_{36}N_6O_6Fe_3B_2$  Calc.: C, 48.6; H, 4.6; N, 10.6; Fe, 21.3%.

### 2.1.5. $FeBd_3(BFc)_2$

This complex was synthesized as previously but  $\alpha$ -benzyl-dioxime (0.72 g, 3 mmol) was used instead of dimethylglyoxime; yield 0.36 g (31%). Anal. Found: C, 63.7; H, 4.0; N, 7.4; Fe, 14.1.  $C_{62}H_{48}N_6O_6Fe_3B_2$  Calc.: C, 64.0; H, 4.1; N, 7.2; Fe, 14.5%.

### 2.1.6. $FeFd_3(BFc)_2$

This complex was synthesized as previously but  $\alpha$ -furyldioxime (0.66 g, 3 mmol) was used instead of  $\alpha$ -benzyl-dioxime; yield 0.28 g (25%). Anal. Found: C, 54.3; H, 3.2; N, 7.3; Fe, 14.8.  $C_{50}H_{36}N_6O_{12}Fe_3B_2$  Calc.: C, 54.5; H, 3.3; N, 7.6; Fe, 15.2%.

### 2.1.7. $FeMm_3(BFc)_2$

This complex was obtained in the same manner as  $FeDm_3(BFc)_2$  except that the reaction mixture was evaporated to dryness and the complex was extracted with 10 ml of chloroform; yield 0.2 g (27%). Anal. Found: C, 46.5; H, 4.1; N, 11.2; Fe, 22.2.  $C_{29}H_{30}N_6O_6Fe_3B_2$  Calc.: C, 46.5; H, 4.0; N, 11.2; Fe, 22.5%.

## 2.2. Crystallographic studies

Single crystals of the  $FeNx_3(BFc)_2 \cdot 2CCl_4$  complex were obtained by slow evaporation of saturated solution in a heptan-carbon tetrachloride (1:1) mixture for several weeks.

A single crystal (0.25 × 0.15 × 0.05 mm) was mounted on a Syntex P1 diffractometer equipped with filtered  $CuK_{\alpha}$  X-ray radiation ( $\lambda = 1.5418 \text{ \AA}$ ). The unit cell parameters and orientation matrix were obtained from the least-squares refinement of the setting angles of centred reflections ( $20^\circ < \theta < 25^\circ$ ).

*Crystal data.*  $C_{40}H_{42}B_2N_6O_6Fe_3Cl_8$ ,  $M = 1175.6$ ,

triclinic, space group  $P\bar{1}$ ,  $a = 10.959(2)$ ,  $b = 14.665(2)$ ,  $c = 17.896(3) \text{ \AA}$ ,  $\alpha = 70.49(1)^\circ$ ,  $\beta = 77.92(1)^\circ$ ,  $\gamma = 69.49(1)^\circ$ ,  $V = 2525.9(09) \text{ \AA}^3$ ,  $Z = 2$ ,  $D_{\text{calc}} = 1.418 \text{ g cm}^{-3}$ ,  $\mu(Cu K_{\alpha}) = 192.81 \text{ cm}^{-1}$ ,  $F(000) = 1192$ . Data were collected by  $\theta/2\theta$  scans up to  $2\theta = 100^\circ$ . 3005 reflections were measured with  $F > 3\sigma(F)$ .

The structure was solved by direct methods and full-matrix least-squares refinement/ $\Delta F$  syntheses (Fe, B, C, N, Cl, O) using SHELXTL [22]. Absorption correction was applied ( $T_{\text{min}} 0.157$ ,  $T_{\text{max}} 0.588$ ). Data were weighted according to  $w^{-1} = [\sigma^2(F) + 0.001134F^2]$ . All non-hydrogen atoms were refined with anisotropic thermal parameters. All hydrogen atoms were refined with given isotropic thermal parameters 0.08 at convergence. Refinement of the structure then proceeded to

Table 2  
Selected bond lengths (Å) in  $FeNx_3(BFc)_2 \cdot 2CCl_4$

Fe(1)–N(1)	1.905(2)	Fe(1)–N(2)	1.921(2)
Fe(1)–N(3)	1.867(2)	Fe(1)–N(4)	1.920(2)
Fe(1)–N(5)	1.926(2)	Fe(1)–N(6)	1.904(2)
Fe(2)–C(19)	2.112(2)	Fe(2)–C(20)	2.030(2)
Fe(2)–C(21)	2.036(2)	Fe(2)–C(22)	2.039(2)
Fe(2)–C(23)	2.043(3)	Fe(2)–C(24)	2.042(2)
Fe(2)–C(25)	2.043(3)	Fe(2)–C(26)	2.016(3)
Fe(2)–C(27)	2.045(2)	Fe(2)–C(28)	2.062(2)
Fe(3)–C(29)	2.068(3)	Fe(3)–C(30)	2.048(2)
Fe(3)–C(31)	2.048(2)	Fe(3)–C(32)	2.046(3)
Fe(3)–C(33)	2.036(3)	Fe(3)–C(34)	1.983(2)
Fe(3)–C(35)	2.015(3)	Fe(3)–C(36)	1.999(3)
Fe(3)–C(37)	1.985(2)	Fe(3)–C(38)	2.090(2)
O(1)–N(1)	1.383	O(1)–B(1)	1.505
O(2)–N(2)	1.359	O(2)–B(1)	1.493
O(3)–N(3)	1.397	O(3)–B(1)	1.466
O(4)–N(4)	1.376	O(4)–B(2)	1.510
O(5)–N(5)	1.349	O(5)–B(2)	1.445
O(6)–N(6)	1.351	O(6)–B(2)	1.509
N(1)–C(1)	1.275	N(2)–C(7)	1.283
N(3)–C(13)	1.341	N(4)–C(12)	1.296
N(5)–C(18)	1.325	N(6)–C(6)	1.304
B(1)–C(19)	1.526	B(2)–C(29)	1.554
C(1)–C(2)	1.521	C(1)–C(6)	1.413
C(2)–C(3)	1.508	C(3)–C(4)	1.488
C(4)–C(5)	1.525	C(5)–C(6)	1.503
C(7)–C(8)	1.478	C(7)–C(12)	1.413
C(8)–C(9a)	1.676	C(8)–C(9b)	1.574
C(9a)–C(9b)	1.152	C(9a)–C(10)	1.281
C(9b)–C(10)	1.341	C(10)–C(11)	1.557
C(11)–C(12)	1.529	C(13)–C(14)	1.499
C(13)–C(18)	1.398	C(14)–C(15)	1.545
C(15)–C(16)	1.430	C(16)–C(17)	1.546
C(17)–C(18)	1.491	C(19)–C(20)	1.405
C(19)–C(23)	1.480	C(20)–C(21)	1.420
C(21)–C(22)	1.410	C(22)–C(23)	1.444
C(24)–C(25)	1.349	C(24)–C(28)	1.446
C(25)–C(26)	1.405	C(26)–C(27)	1.365
C(27)–C(28)	1.419	C(29)–C(30)	1.436
C(29)–C(33)	1.381	C(30)–C(31)	1.464
C(31)–C(32)	1.360	C(32)–C(33)	1.398
C(34)–C(35)	1.395	C(34)–C(38)	1.429
C(35)–C(36)	1.327	C(36)–C(37)	1.327
C(37)–C(38)	1.445		

Table 3  
Selected bond angles (°) in  $\text{FeN}_x_3(\text{BFC})_2 \cdot 2\text{CCl}_4$

N(1)–Fe(1)–N(2)	84.5(1)	N(1)–Fe(1)–N(3)	87.8(1)
N(2)–Fe(1)–N(3)	84.0(1)	N(1)–Fe(1)–N(4)	125.9(1)
N(2)–Fe(1)–N(4)	77.3(1)	N(3)–Fe(1)–N(4)	138.7(1)
N(1)–Fe(1)–N(5)	144.4(1)	N(2)–Fe(1)–N(5)	126.2(1)
N(3)–Fe(1)–N(5)	79.2(1)	N(4)–Fe(1)–N(5)	82.8(1)
N(1)–Fe(1)–N(6)	77.4(1)	N(2)–Fe(1)–N(6)	140.3(1)
N(3)–Fe(1)–N(6)	129.5(1)	N(4)–Fe(1)–N(6)	85.2(1)
N(5)–Fe(1)–N(6)	85.6(1)	C(19)–Fe(2)–C(20)	39.6
C(19)–Fe(2)–C(21)	68.3(1)	C(20)–Fe(2)–C(21)	40.9
C(19)–Fe(2)–C(22)	69.9(1)	C(20)–Fe(2)–C(22)	68.8(1)
C(21)–Fe(2)–C(22)	40.5	C(19)–Fe(2)–C(23)	41.7
C(20)–Fe(2)–C(23)	68.2(1)	C(21)–Fe(2)–C(23)	68.4(1)
C(22)–Fe(2)–C(23)	41.4(1)	C(19)–Fe(2)–C(24)	107.7(1)
C(20)–Fe(2)–C(24)	121.7(1)	C(21)–Fe(2)–C(24)	157.0(1)
C(22)–Fe(2)–C(24)	161.6(1)	C(23)–Fe(2)–C(24)	124.8(1)
C(19)–Fe(2)–C(25)	123.6(1)	C(20)–Fe(2)–C(25)	109.1(1)
C(21)–Fe(2)–C(25)	123.4(1)	C(22)–Fe(2)–C(25)	157.7(1)
C(23)–Fe(2)–C(25)	160.1(1)	C(24)–Fe(2)–C(25)	38.6
C(19)–Fe(2)–C(26)	160.8(1)	C(20)–Fe(2)–C(26)	126.3(1)
C(21)–Fe(2)–C(26)	109.4(1)	C(22)–Fe(2)–C(26)	121.7(1)
C(23)–Fe(2)–C(26)	156.9(1)	C(24)–Fe(2)–C(26)	66.4(1)
C(25)–Fe(2)–C(26)	40.5(1)	C(19)–Fe(2)–C(27)	157.9(1)
C(20)–Fe(2)–C(27)	161.1(1)	C(21)–Fe(2)–C(27)	124.0(1)
C(22)–Fe(2)–C(27)	106.8(1)	C(23)–Fe(2)–C(27)	121.5(1)
C(24)–Fe(2)–C(27)	68.2(1)	C(25)–Fe(2)–C(27)	67.6(1)
C(26)–Fe(2)–C(27)	39.3	C(19)–Fe(2)–C(28)	122.2(1)
C(20)–Fe(2)–C(28)	157.3(1)	C(21)–Fe(2)–C(28)	160.2(1)
C(22)–Fe(2)–C(28)	123.5(1)	C(23)–Fe(2)–C(28)	107.3(1)
C(24)–Fe(2)–C(28)	41.3	C(25)–Fe(2)–C(28)	67.2(1)
C(26)–Fe(2)–C(28)	66.6(1)	C(27)–Fe(2)–C(28)	40.4
C(29)–Fe(3)–C(30)	40.9	C(29)–Fe(3)–C(31)	68.4(1)
C(30)–Fe(3)–C(31)	42.0	C(29)–Fe(3)–C(32)	68.2(1)
C(30)–Fe(3)–C(32)	68.7(1)	C(31)–Fe(3)–C(32)	38.8
C(29)–Fe(3)–C(33)	39.3(1)	C(30)–Fe(3)–C(33)	67.0(1)
C(31)–Fe(3)–C(33)	65.7(1)	C(32)–Fe(3)–C(33)	40.1(1)
C(29)–Fe(3)–C(34)	111.0(1)	C(30)–Fe(3)–C(34)	129.1(1)
C(31)–Fe(3)–C(34)	167.3(2)	C(32)–Fe(3)–C(34)	153.7(2)
C(33)–Fe(3)–C(34)	122.5(1)	C(29)–Fe(3)–C(35)	120.1(1)
C(30)–Fe(3)–C(35)	107.2(1)	C(31)–Fe(3)–C(35)	127.6(2)
C(32)–Fe(3)–C(35)	163.3(2)	C(33)–Fe(3)–C(35)	154.8(1)
C(34)–Fe(3)–C(35)	40.8(1)	C(29)–Fe(3)–C(36)	151.4(1)
C(30)–Fe(3)–C(36)	116.7(1)	C(31)–Fe(3)–C(36)	107.6(1)
C(32)–Fe(3)–C(36)	127.4(1)	C(33)–Fe(3)–C(36)	166.5(1)
C(34)–Fe(3)–C(36)	66.5(1)	C(35)–Fe(3)–C(36)	38.6(1)
C(29)–Fe(3)–C(37)	169.0(2)	C(30)–Fe(3)–C(37)	149.1(2)
C(31)–Fe(3)–C(37)	116.4(1)	C(32)–Fe(3)–C(37)	108.8(1)
C(33)–Fe(3)–C(37)	131.8(1)	C(34)–Fe(3)–C(37)	66.7(1)
C(35)–Fe(3)–C(37)	65.9(1)	C(36)–Fe(3)–C(37)	38.9(1)
C(29)–Fe(3)–C(38)	129.6(1)	C(30)–Fe(3)–C(38)	167.7(1)
C(31)–Fe(3)–C(38)	149.3(1)	C(32)–Fe(3)–C(38)	117.9(1)
C(33)–Fe(3)–C(38)	110.6(1)	C(34)–Fe(3)–C(38)	41.0
C(35)–Fe(3)–C(38)	69.5(1)	C(36)–Fe(3)–C(38)	68.7(1)
C(37)–Fe(3)–C(38)	41.4	N(1)–O(1)–B(1)	114.8
N(2)–O(2)–B(1)	114.1	N(3)–O(3)–B(1)	114.3
N(4)–O(4)–B(2)	114.2	N(5)–O(5)–B(2)	114.0
N(6)–O(6)–B(2)	115.1	Fe(1)–N(1)–O(1)	123.5
Fe(1)–N(1)–C(1)	119.1(1)	O(1)–N(1)–C(1)	117.3
Fe(1)–N(2)–O(2)	125.0(1)	Fe(1)–N(2)–C(7)	119.2(1)
O(2)–N(2)–C(7)	115.6	Fe(1)–N(3)–O(3)	124.4(1)
Fe(1)–N(3)–C(13)	119.7(1)	O(3)–N(3)–C(13)	115.6
Fe(1)–N(4)–O(4)	123.6(1)	Fe(1)–N(4)–C(12)	118.6(1)
O(4)–N(4)–C(12)	117.8	Fe(1)–N(5)–O(5)	126.1(1)
Fe(1)–N(5)–C(18)	115.9(1)	O(5)–N(5)–C(18)	117.9
Fe(1)–N(6)–O(6)	124.4(1)	Fe(1)–N(6)–C(6)	119.2(1)

Table 3 (continued)

O(6)–N(6)–C(6)	116.1	O(1)–B(1)–O(2)	105.1
O(1)–B(1)–O(3)	109.1	O(2)–B(1)–O(3)	110.4
O(1)–B(1)–C(19)	107.9	O(2)–B(1)–C(19)	114.5
O(3)–B(1)–C(19)	109.6	O(4)–B(2)–O(5)	110.5
O(4)–B(2)–O(6)	105.6	O(5)–B(2)–O(6)	108.9
O(4)–B(2)–C(29)	106.2	O(5)–B(2)–C(29)	113.6
O(6)–B(2)–C(29)	111.7	N(1)–C(1)–C(2)	124.5
N(1)–C(1)–C(6)	113.1	C(2)–C(1)–C(6)	122.1
C(1)–C(2)–C(3)	111.3	C(2)–C(3)–C(4)	111.7
C(3)–C(4)–C(5)	113.8	C(4)–C(5)–C(6)	110.3
N(6)–C(6)–C(1)	110.9	N(6)–C(6)–C(5)	126.2
C(1)–C(6)–C(5)	122.9	N(2)–C(7)–C(8)	126.1
N(2)–C(7)–C(12)	112.4	C(8)–C(7)–C(12)	121.5
C(7)–C(8)–C(9a)	105.9	C(7)–C(8)–C(9b)	106.8
C(9a)–C(8)–C(9b)	41.4	C(8)–C(9a)–C(9b)	64.6
C(8)–C(9a)–C(10)	114.3	C(9b)–C(9a)–C(10)	66.6
C(8)–C(9a)–C(9a)	74.0	C(8)–C(9b)–C(10)	117.4
C(9a)–C(9b)–C(10)	61.3	C(9a)–C(10)–C(9b)	52.1
C(9a)–C(10)–C(11)	118.7	C(9b)–C(10)–C(11)	119.0
C(10)–C(11)–C(12)	107.2	N(4)–C(12)–C(7)	112.5
N(4)–C(12)–C(11)	121.1	C(7)–C(12)–C(11)	126.4
N(3)–C(13)–C(14)	124.7	N(3)–C(13)–C(18)	110.3
C(14)–C(13)–C(18)	125.0	C(13)–C(14)–C(15)	106.7
C(14)–C(15)–C(16)	116.0	C(15)–C(16)–C(17)	113.6
C(16)–C(17)–C(18)	110.3	N(5)–C(18)–C(13)	114.6
N(5)–C(18)–C(17)	122.0	C(13)–C(18)–C(17)	123.2
Fe(2)–C(19)–B(1)	133.5(1)	Fe(2)–C(19)–C(20)	67.1(1)
B(1)–C(19)–C(20)	131.1	Fe(2)–C(19)–C(23)	66.6(1)
B(1)–C(19)–C(23)	124.2	C(20)–C(19)–C(23)	104.5
Fe(2)–C(20)–C(19)	73.3(1)	Fe(2)–C(20)–C(21)	69.8(1)
C(19)–C(20)–C(21)	111.1	Fe(2)–C(21)–C(20)	69.3(1)
Fe(2)–C(21)–C(22)	69.9(1)	C(20)–C(21)–C(22)	108.6
Fe(2)–C(22)–C(21)	69.7(1)	Fe(2)–C(22)–C(23)	69.4(1)
C(21)–C(22)–C(23)	106.9	Fe(2)–C(23)–C(19)	71.7
Fe(2)–C(23)–C(22)	69.1(1)	C(19)–C(23)–C(22)	108.8
Fe(2)–C(24)–C(25)	70.8(1)	Fe(2)–C(24)–C(28)	70.1(1)
C(25)–C(24)–C(28)	108.7	Fe(2)–C(25)–C(24)	70.7(1)
Fe(2)–C(25)–C(26)	68.7(1)	C(24)–C(25)–C(26)	107.6
Fe(2)–C(26)–C(25)	70.8(1)	Fe(2)–C(26)–C(27)	71.5(1)
C(25)–C(26)–C(27)	110.5	Fe(2)–C(27)–C(26)	69.2(1)
Fe(2)–C(27)–C(28)	70.5(1)	C(26)–C(27)–C(28)	107.0
Fe(2)–C(28)–C(24)	68.6(1)	Fe(2)–C(28)–C(27)	69.1(1)
C(24)–C(28)–C(27)	106.1	Fe(3)–C(29)–B(2)	129.6(1)
Fe(3)–C(29)–C(30)	68.4(1)	B(2)–C(29)–C(30)	124.4
Fe(3)–C(29)–C(33)	69.1(1)	B(2)–C(29)–C(33)	129.5
C(30)–C(29)–C(33)	106.0	Fe(3)–C(30)–C(29)	70.7(1)
Fe(3)–C(30)–C(31)	69.4(1)	C(29)–C(30)–C(31)	105.8
Fe(3)–C(31)–C(30)	68.6(1)	Fe(3)–C(31)–C(32)	70.6(1)
C(30)–C(31)–C(32)	109.3	Fe(3)–C(32)–C(31)	70.6(1)
Fe(3)–C(32)–C(33)	69.6(1)	C(31)–C(32)–C(33)	106.8
Fe(3)–C(33)–C(29)	71.6(1)	Fe(3)–C(33)–C(32)	70.4(1)
C(29)–C(33)–C(32)	112.1	Fe(3)–C(34)–C(35)	70.8(1)
Fe(3)–C(34)–C(38)	73.5(1)	C(35)–C(34)–C(38)	111.9
Fe(3)–C(35)–C(34)	68.3(1)	Fe(3)–C(35)–C(36)	70.0(1)
C(34)–C(35)–C(36)	106.5	Fe(3)–C(36)–C(35)	71.4(1)
Fe(3)–C(36)–C(37)	70.0(1)	C(35)–C(36)–C(37)	110.1
Fe(3)–C(37)–C(36)	71.1(1)	Fe(3)–C(37)–C(38)	73.2(1)
C(36)–C(37)–C(38)	112.6	Fe(3)–C(38)–C(34)	65.5(1)
Fe(3)–C(38)–C(37)	65.4(1)	C(34)–C(38)–C(37)	98.8

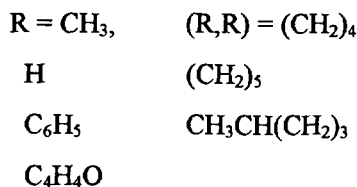
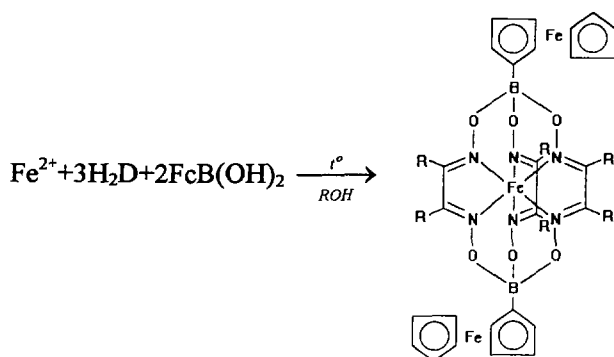
$R = 0.089$  and  $R_w = 0.04$ . Atomic scattering factors for Fe, B, Cl, C, N and O were inlaid in SHELXTL [24]. One cyclohexane ring ( $\text{C}_7\text{--C}_{12}$ ) in the dioxime moiety is

statistically disordered in the region of the C9 atom (Table 1, C9a and C9b) with 50% probability. For two disordered carbon tetrachloride molecules only carbon atom coordinates are presented, but eight chlorine atoms have been taken into consideration in calculations. The atomic coordinates and bond distances and angles are presented in Tables 1–3. Anisotropic displacement parameters, hydrogen atom coordinates, and a complete list of bond lengths and angles have been deposited at the Cambridge Crystallographic Data Centre.

### 3. Results and discussion

#### 3.1. Synthesis

Trinuclear macrobicyclic iron(II) complexes with acyclic, aromatic and alicyclic dioximes, listed in Fig. 1, have been synthesized by direct template reactions on the  $\text{Fe}^{2+}$  ion using ferrocenylboric acid as the cross-linking agent:



As could be expected, the complexes with alicyclic dioximes, which have only *cis*-conformation, have been formed most readily. The synthesis of acyclic and aromatic dioxime complexes occurs under much more rigid conditions and involves neutralization of the  $\text{H}^+$  ions released in the course of reaction and, in some cases, azeotropic distillation of water. Unfortunately, we failed to isolate the complex of the glyoxime. All attempts to replace the solvent and change the synthesis conditions were unsuccessful.

#### 3.2. Spectra and structure

$^{57}\text{Fe}$  Mössbauer spectroscopy proved to be a unique tool in studying the spatial and electronic structure of iron complexes. The parameters of the  $^{57}\text{Fe}$  Mössbauer data have been used to determine the structure of low-spin iron(II) clathrochelates [6]. The fact that the isomeric shift (IS) value determined by the *s*-electron density of the iron nucleus is lower than the calculated one has been attributed to the 'macrocyclic' effect of the ligand field increase. A similar effect has been observed for all synthesized compounds. According to Bancroft's partial isomeric shift (PIS) concept [25], the expected IS value for the central iron atom in the nioxime compound (ca.  $0.40 \text{ mm s}^{-1}$ ) is appreciably higher than the experimentally observed one (Table 4). In addition to the lines assigned to low-spin central iron(II) atoms, the spectra contain doublet signals for the iron atoms of ferrocenylboron cross-linking fragments.

Some peculiarities of the central iron(II) atom nearest environment geometry, intermediates between trigonal prismatic (TP) and trigonal antiprismatic (TAP) (Fig. 2), have been defined from the correlation dependences of the quadrupole splitting (QS), determined by the electric field gradient on the iron atom nucleus, and the  $t_{2g}$  level splitting versus coordination polyhedron distortion angle  $\varphi$  [6]. The validity of this approach has been confirmed by the X-ray analysis data obtained for a wide range of new iron(II) clathrochelates. In the case of the TP coordination polyhedron ( $\varphi = 0^\circ$ ), QS values are high (ca.  $1 \text{ mm s}^{-1}$ ) and have a positive sign (the  $e_g$  level energy is higher than the  $a_{1g}$  level energy). For TAP complexes ( $\varphi = 60^\circ$ ), the QS values are small and negative (the  $a_{1g}$  level energy is higher than the  $e_g$  level energy). The QS values in the spectra for ferrocenylborate clathrochelates belonging to the central iron atom are rather high and clearly positive. Thus, the geometry of the synthesized complexes may be estimated with high accuracy using the QS values and the new approach to the partial quadrupole splitting (PQS) concept [26]. In accordance with this approach, QS is described by the equation

$$\text{QS} = f \times (\text{PQS}) \quad (1)$$

where  $f$  is a function of the iron ion coordination environment geometry and may be expressed as

$$f = 12 - 18 \cos^2 \alpha / \cos^2 (\varphi/2) \quad (2)$$

The PQS value for complexes of this type is ca.  $0.5 \text{ mm s}^{-1}$  [26]. The calculated and experimentally obtained QS values for a series of compounds with known geometry are listed in Table 5. It is obvious that the difference between the experimental and calculated QS

Table 4  
 ( $^1\text{H}$ ,  $^{13}\text{C}$ ( $^1\text{H}$ ),  $^{11}\text{B}$ ) NMR (ppm) and ( $^{57}\text{Fe}$ ) Mössbauer ( $\text{mm s}^{-1}$ ) data

Compound	$^1\text{H}$ relative TMS		$^{13}\text{C}$ relative TMS			$^{11}\text{B}$ relative $\text{NaB}(\text{C}_6\text{H}_5)_4$	$^{57}\text{Fe}$		Predicted $\varphi$ value ( $^\circ$ )
	H–C=N	R	H–C=N	R–C=N	R		IS	QS	
$\text{FeMm}_3(\text{BFc})_2$	7.70	2.42	141.54	149.66	13.64		0.30	0.50	19–25
			141.77	149.99			0.69	2.35	
			141.99	150.12					
$\text{FeDm}_3(\text{BFc})_2$		2.41		151.02	13.19		0.31	0.58	14–20
$\text{FeBd}_3(\text{BFc})_2$		8.66 m		158.60	127.65		0.70	2.35	
					129.33		0.34	0.40	
					130.01		0.71	2.41	
					130.85				
$\text{FeFd}_3(\text{BFc})_2$		6.50		146.43	111.88	13.2	0.34	0.35	25–3 <sup>1</sup>
					118.55		0.69	2.29	
					144.70				
					145.30				
$\text{H}_2\text{Fd}$		6.60 m		141.142	112.3				
		7.60 m		117.45					
					143.28				
					145.28				
$\text{FeFd}_3(\text{BBu})_2$		6.54		145.16	111.64	14.8	0.28	0.10	
		7.27			118.36				
					142.19				
					143.63				
$\text{FeNx}_3(\text{BFc})_2$		1.80		150.84	21.61		0.31	0.72	9.5 <sup>a</sup>
		2.94			26.09		0.70	2.36	
$\text{Fe}(4\text{MNx})_3(\text{BFc})_2$		1.10–3.5 m		150.67	21.16		0.31	0.62	11–17
				150.96	25.31		0.70	2.35	
					28.55				
					29.78				
					33.98				
$\text{FeGx}_3(\text{BFc})_2$		1.78 m		157.66	25.54		0.31	0.47	20–26
					27.10		0.70	2.37	
		3.09			30.71				

<sup>a</sup> X-ray structure data.

values depends on the nature of the cross-linking group. Therefore, having estimated the contribution of a cross-linking fragment to the QS magnitude for one of the compounds of the series, one can evaluate the distortion angles for the rest of them. The X-ray analysis of the  $\text{FeNx}_3(\text{BFc})_2 \cdot 2\text{CCl}_4$  complex has permitted us to determine the effect of a ferrocenylboron cross-linking fragment on the QS magnitude. The main parameters of the central iron(II) coordination polyhedron (Fe–N distance ca. 1.9 Å and N–Fe–N bite (chelate) angle ca.

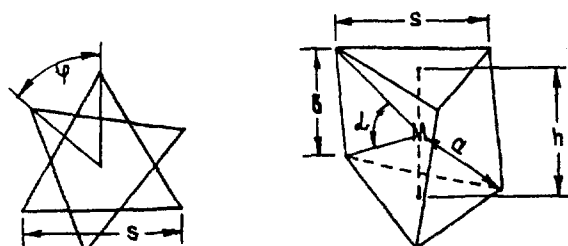


Fig. 2. The TAP–TP coordination polyhedron.

39°) are characteristic of macrobicyclic compounds of this type. The smallest distortion angle value ( $\varphi$  ca. 9.5°) due to steric hindrance arising between the bulky ferrocenyl substituents and the cyclohexane ring is responsible for increasing the distance between the trigonal prism bases up to 2.38 Å (Figs. 3 and 4).

The difference between the calculated and experimentally observed QS values ( $0.14 \text{ mm s}^{-1}$ , Table 5) has been employed to predict  $\varphi$  values for the other synthesized complexes at  $\alpha = 39^\circ$ . The  $\varphi$  value can be evaluated by the equations

$$\text{QS} - f \times \text{PQS} = 0.14$$

$$f = 12 - 18 \cos^2 39^\circ / \cos^2 (\varphi/2)$$

and therefore  $\varphi = 2 \arccos(3 \cos 39^\circ / \sqrt{6.14 - \text{QS}})$ . As follows from Table 4 data, the magnitude of  $\alpha$  is usually within  $39 \pm 0.3^\circ$ , which implies that the distortion angle value has been determined with an accuracy of  $\pm 3^\circ$ . The calculated  $\varphi$  values for a series of ferrocenylborate complexes are listed in Table 4. A compari-

Table 5

The quadrupole splittings QS ( $\text{mm s}^{-1}$ ), bite  $\alpha$  and twist  $\varphi$  angles ( $^\circ$ ), Fe–N bond lengths  $a$ , base spacings  $h$  ( $\text{\AA}$ ) and PQS values ( $\text{mm s}^{-1}$ ) calculated from Eq. (1) for macrobicyclic iron complexes

Compound	$a$	$h$	QS <sup>a</sup>	$\alpha$	$\varphi$	$f$	$f \times \text{PQS}$	QS – $f \times \text{PQS}$	Reference
FePhm <sub>3</sub> (BC <sub>6</sub> H <sub>5</sub> ) <sub>2</sub> · BF <sub>3</sub>	1.91	2.34	(+)0.48	39.2	21.8	0.79	0.40	+0.1	[27]
FeBd <sub>3</sub> (BF) <sub>2</sub> · 5CHCl <sub>3</sub>	1.91	2.39	(+)0.28	39.3	29.3	0.49	0.20	+0.1	[28]
FeFd <sub>3</sub> (BC <sub>6</sub> H <sub>5</sub> ) <sub>2</sub> · 1/4CHCl <sub>3</sub>	1.91	2.31	0.0	39.2	26.4	0.60	0.24	–0.2	[10]
FeGx <sub>3</sub> (BOH) <sub>2</sub> · 3H <sub>2</sub> O	1.91	2.33	(+)0.50	39.1	23.4	0.70	0.35	+0.1	[29]
FeGx <sub>3</sub> (BC <sub>6</sub> H <sub>5</sub> ) <sub>2</sub> · 2CHCl <sub>3</sub>	1.915	2.35	(+)0.50	38.9	20.2	0.75	0.38	+0.1	[30]
FeDm <sub>3</sub> (BF) <sub>2</sub>	1.92	<sup>b</sup>	(+)0.90	39	16.5	1.18	0.60	+0.3	[1]
FeNx <sub>3</sub> (SnCl <sub>3</sub> ) <sub>2</sub> <sup>–</sup>	1.92	2.23	(–)0.19	39.5	37.5	0.04	0.02	–0.2	[31]
FeGm <sub>3</sub> (Bn–C <sub>4</sub> H <sub>9</sub> ) <sub>2</sub>	1.92	2.39	(+)0.84	38.6	10.9	0.90	0.50	+0.3	[10]
[FePcc(BF)] <sup>+</sup>	1.91	<sup>b</sup>	+0.95	39.5	21.8	0.90	0.50	+0.4	[32]
FeNx <sub>3</sub> (BFc) <sub>2</sub> · 2CCl <sub>4</sub>	1.90	2.38	(+)0.72	39.3	9.5	1.16	0.58	+0.14	<sup>c</sup>

<sup>a</sup> Values of QS were obtained at X-ray structure analyses temperatures.

<sup>b</sup> The data is absent.

<sup>c</sup> This work.

son of the Mössbauer spectra parameters for synthesized compounds and other boron-containing clathrochelate iron(II) dioximates suggests that the coordination polyhedra of their central atoms have identical structure. As a consequence, the parameters of the electronic absorption spectra are also close: asymmetrical charge transfer bands (CTBs) dominate in the visible region, whose

components have been obtained from a second-order spectra derivative (Table 6). The intensive ( $\epsilon \sim 10^3$ – $10^4 \text{ mol}^{-1} \text{ dm}^3 \text{ cm}^{-1}$ ) bands mask the bands of  $^1A_{1g} \rightarrow ^3E_{1g}$ ,  $^1E_{1g}$ ,  $^2E_{1g}$   $d$ – $d$  transitions from 18000 to 30000  $\text{cm}^{-1}$  characteristic of ferrocenyl derivatives [33]. At the same time, these substituents are readily detectable in the IR and  $^1\text{H}$ ,  $^{13}\text{C}\{^1\text{H}\}$  NMR spectra. Apart

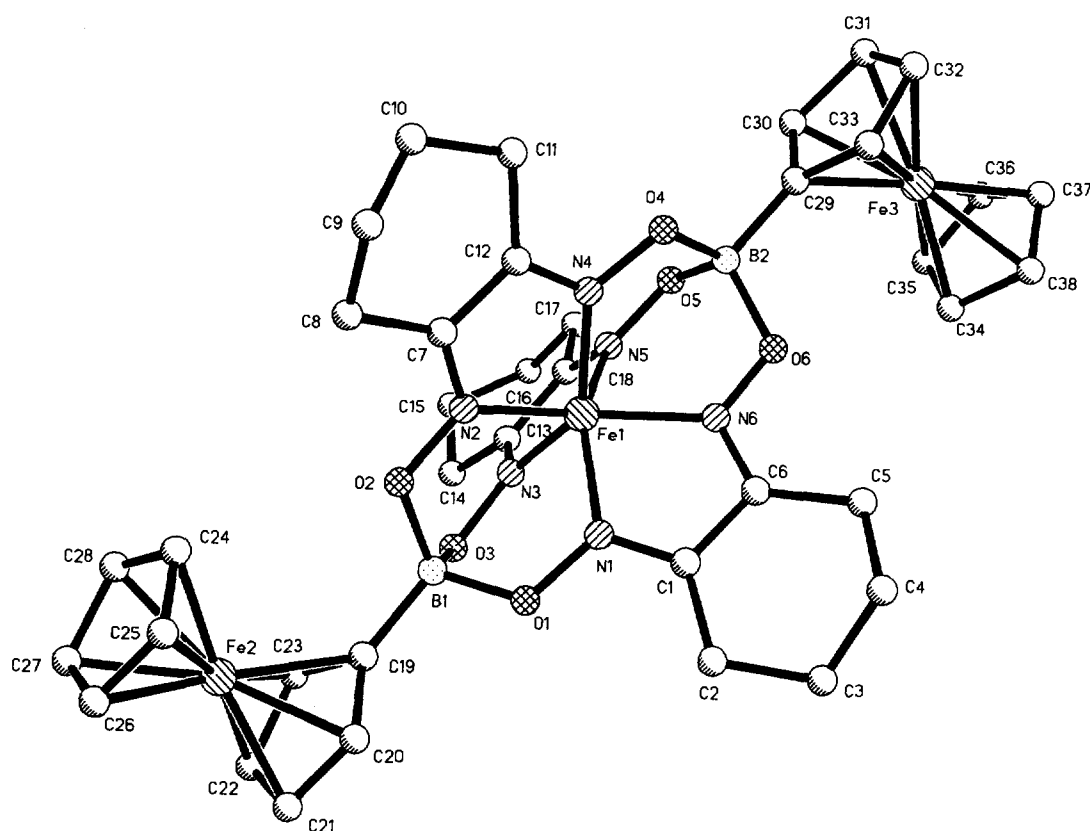


Fig. 3. Perspective view of an FeNx<sub>3</sub>(BFc)<sub>2</sub> molecule with the labelling scheme used.

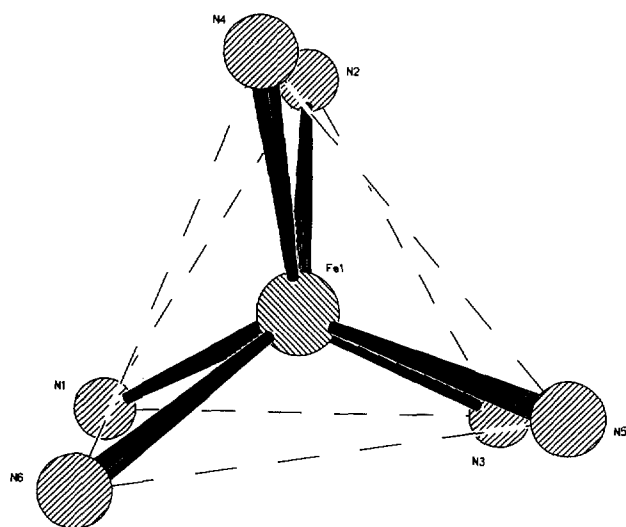


Fig. 4. The iron(II) coordination polyhedron in the  $\text{FeNx}_3(\text{BFc})_2$  molecule.

from the cyclopentadienyl ring  $\nu(\text{C-H})$  bands at  $3100\text{ cm}^{-1}$ , the IR spectra for the synthesized compounds also contain an intense stretching vibration band at ca.  $480\text{ cm}^{-1}$  and related calculation bands of the cyclopentadienyl ring at ca.  $500\text{ cm}^{-1}$  as well as the C–C vibration of the ring at  $1100$  and  $1430\text{--}1460\text{ cm}^{-1}$ . The vibrations in the cyclopentadienyl ring have manifested themselves at  $800\text{--}850\text{ cm}^{-1}$  [34]. Moreover, the stretching vibrations of a clathrochelate fragment active in the IR spectra (the stretching vibrations of the C=N and N–O bonds) are registered at the same frequencies as for the rest of the macrobicyclic iron dioximates. In this case, for certain dioximates the  $\nu(\text{C=H})$  band

doubles. Intense B–O bond stretching vibration bands for the tetrahedral ferrocenylborate fragment have been observed at  $1100\text{--}1200\text{ cm}^{-1}$ .

The  $^1\text{H}$  and  $^{13}\text{C}\{^1\text{H}\}$  NMR spectra for the synthesized compounds (Table 4), alongside the lines belonging to the macrobicyclic dioximate framework, show the signals for a ferrocenyl substituent at the tetrahedral boron atoms ( $\delta_{\text{H}} \sim 13\text{ ppm}$ ): three signals with a 2:2:5 intensity ratio ( $\delta_{\text{H}}$  between 4 and 4.5 ppm and  $\delta_{^{13}\text{C}}$  between 68 and 72 ppm). The most intense signal, being in the strong field with respect to the two other signs, is attributed to an unsubstituted cyclopentadienyl ring.

For non-symmetrical methylglyoximate  $\text{FeMm}_3(\text{BFc})_2$  complex, both *fac*- and *mer*-isomers in a static ratio 1:3 were detected from the  $^{13}\text{C}\{^1\text{H}\}$  NMR spectrum (Fig. 5). Each signal from the azomethine carbon atoms of both types (substituted and unsubstituted) consists of three lines, two of them refer to the *mer*-isomer and the third to the *fac*-isomer, which has  $\text{C}_3$  symmetry. The ferrocene-containing fragment lines also becomes magnetically non-equivalent.

Fig. 6 illustrates a typical cyclic voltammogram of the  $\text{FeGx}_3(\text{BFc})_2$  complex in dichloromethane. Half-wave potentials for the complexes under study are listed in Table 7. The results obtained in acetonitrile or dichloromethane are similar. Normally, the voltammograms include two waves, both reversible with a Tomeš criterion of ca. 60 mV and a distance between them of  $855 \pm 20\text{ mV}$ . The first and more intensive wave can be referred to the oxidation of two independent ferrocenylboron-containing fragments in a complex. A notable shift of  $100\text{--}200\text{ mV}$  to the cathode range versus the  $\text{Fc}^+/\text{Fc}$  potential is obviously caused by donor substitution in cyclopentadienyl rings in complexes.

Table 6  
Characteristics of electronic ( $\times 10^{-3}\text{ cm}^{-1}$ ) and IR ( $\text{cm}^{-1}$ ) spectra

Compound	$\nu_1$	$\nu_2$	$\nu_3$	$\nu_1(\text{C=N})$	$\nu_1(\text{N-O})$	$\nu_1(\text{B-O})$
$\text{FeMm}_3(\text{BFc})_2$	22.51	23.81	28.56sh	1561 1572	948, 980 1050, 1062 1238	1147vs
$\text{FeDm}_3(\text{BFc})_2$	22.52	23.25sh	28.49sh	1579	920, 1062 1235	1203vs
$\text{FeBd}_3(\text{BFc})_2$	19.43 20.69	24.03	29.55	1579 1600	896, 1052 1230	1105vs
$\text{FeFd}_3(\text{BFc})_2$	19.25 20.15	25.00sh	31.90	1580m 1580m	932, 1020 1058, 1236	1116vs
$\text{FeNx}_3(\text{BFc})_2$	22.16	23.81	28.57sh	1562 1582	910, 934 1050, 1067 1233	1203vs
$\text{Fe(4MNx)}_3(\text{BFc})_2$	22.16	3.98	28.57sh	1579	925, 1050 1062, 1233	1199vs
$\text{FeGx}_3(\text{BFc})_2$	22.36	22.64	28.57sh	1560 1576	920, 933 1050, 1062 1232	1173vs
$\text{FeFd}_3(\text{BBu})_2$	19.19 20.03	25.00sh	31.80	1584	947, 1074 1230	1210s



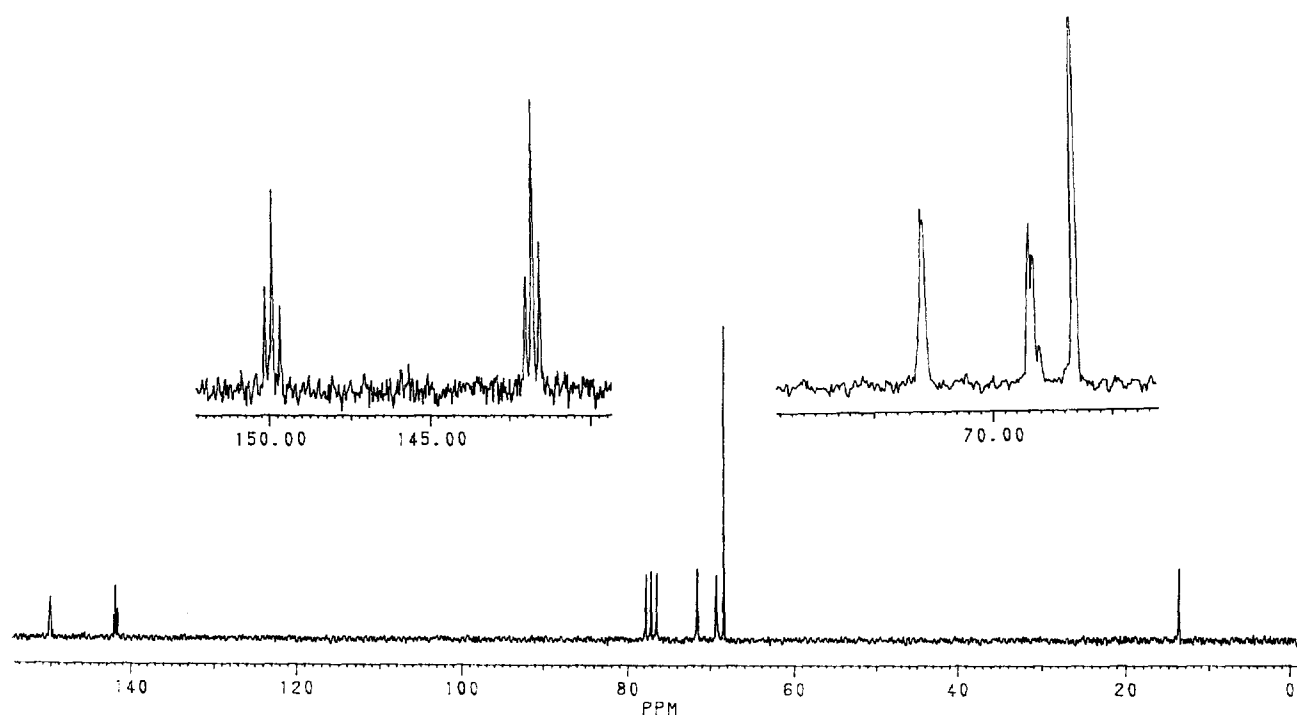


Fig. 5. The  $^{13}\text{C}\{^1\text{H}\}$  NMR spectrum of the  $\text{FeMm}_3(\text{BFc})_2$  complex solution in  $\text{CDCl}_3$ .

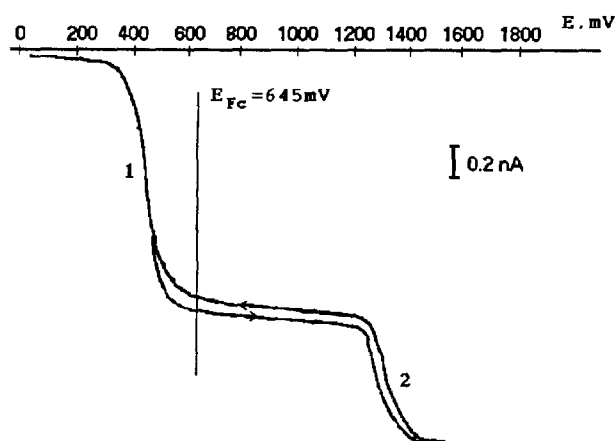


Fig. 6. Cyclic voltammogram of the  $\text{FeGx}_3(\text{BFc})_2$  complex in  $\text{CH}_2\text{Cl}_2$  at  $[(\text{Bu}_4\text{N})\text{BF}_4] = 0.1 \text{ mol dm}^{-3}$ .

The second wave, which appears at higher potentials, by its intensity and position [13] can be referred to the oxidation of central encapsulated iron(II) ion. Both the potentials of the two waves and the distance between them are practically independent of the solvent. This can be accounted for by a weak interaction of all three iron ions in complexes with solvent molecules. Obviously, the interaction between iron ions within a trinuclear complex is negligible as well. However, in complexes with bulky substituents, e.g. furyl or phenyl, both waves become quasi-reversible, and the distance between them decreases. In our opinion, this reflects steric interactions between the redox centres within these complexes.

Table 7

Electrochemical characteristics of trinuclear iron(II) clathrochelate dioximates with ferrocenylboron fragments ( $E_{1/2}$  vs.  $\text{Fc}^+/\text{Fc}$ )

Compound	Acetonitrile			Dichloromethane		
	$E_{1/2}$ (mV)	$E_{1/2}$ (mV)	Tomeš criterion	$E_{1/2}$ (mV)	$E_{1/2}$ (mV)	Tomeš criterion
$\text{FeGx}_3(\text{BFc})_2$	-125	742	60;60	-210	665	65;65
$\text{FeNx}_3(\text{BFc})_2$	-125	742	60;60	-162	713	65;65
$\text{Fe}(\text{MNx})_3(\text{BFc})_2$	-125	742	60;60	-185	720	65;65
$\text{FeMm}_3(\text{BFc})_2$	-105	<sup>a</sup>	60; <sup>a</sup>	-185	950 <sup>a</sup>	65; <sup>a</sup>
$\text{FeDm}_3(\text{BFc})_2$	-130	770	60;60	-170	710	65;65
$\text{FeFd}_3(\text{BFc})_2$	-50	656	87;132	-120	585	65;200
$\text{FeBd}_3(\text{BFc})_2$	-146	549	64;110	-215	565	70;110

<sup>a</sup> The second wave appears as a peak at scan rates of at least  $10 \text{ mV s}^{-1}$ . This process passivates the electrode and the reaction becomes irreversible.

## Acknowledgements

The support of the International Science Foundation (Soros Grants U5C000 and N8L000) and the Russian Foundation of Fundamental Researches is gratefully acknowledged.

## References

- [1] S.C. Jackels and N.J. Rose, *Inorg. Chem.*, **12** (1972) 1232.
- [2] A.Yu. Nazarenko and Ya.Z. Voloshin, *Zh. Neorg. Khim.*, **28** (1984) 1776.
- [3] Ya.Z. Voloshin, A.Yu. Nazarenko and V.V. Trachevskii, *Ukr. Khim. Zh.*, **51** (1985) 121.
- [4] Ya.Z. Voloshin, N.A. Kostromina, A.Yu. Nazarenko and E.V. Polshin, *Ukr. Khim. Zh.*, **55** (1989) 7.
- [5] Ya.Z. Voloshin, A.Yu. Nazarenko, N.A. Kostromina and V.N. Shuman, *Ukr. Khim. Zh.*, **56** (1990) 1238.
- [6] Ya.Z. Voloshin, N.A. Kostromina and A.Yu. Nazarenko, *Inorg. Chim. Acta*, **170** (1990) 181.
- [7] Ya.Z. Voloshin, A.Yu. Nazarenko, E.V. Polshin, S.I. Tyukhtenko and N.A. Kostromina, *Theor. Exp. Khim.*, **25** (1989) 322.
- [8] Ya.Z. Voloshin, N.A. Kostromina, A.Yu. Nazarenko and E.V. Polshin, *Inorg. Chim. Acta*, **185** (1991) 83.
- [9] Ya.Z. Voloshin and E.V. Polshin, *Polyhedron*, **11** (1992) 457.
- [10] S.V. Lindeman, Yu.T. Struchkov and Ya.Z. Voloshin, *Polish J. Chem.*, **67** (1993) 1575.
- [11] Ya.Z. Voloshin, V.V. Trachevskii and E.V. Polshin, *J. Coord. Chem.*, in press.
- [12] M.K. Robbins, D.W. Naser, J.L. Heiland and J.J. Grzybowski, *Inorg. Chem.*, **24** (1985) 3381.
- [13] V.V. Strelets, S.V. Kukharenko and Ya.Z. Voloshin, *Polish J. Chem.*, **69** (1995) 1520.
- [14] D.R. Boston and N.J. Rose, *J. Am. Chem. Soc.*, **95** (1973) 4163.
- [15] Ya.Z. Voloshin, N.A. Kostromina and A.Yu. Nazarenko, *Theor. Exp. Khim.*, **26** (1990) 375.
- [16] Ya.Z. Voloshin, V.K. Belsky and V.V. Trachevskii, *Polyhedron*, **11** (1992) 1939.
- [17] Ya.Z. Voloshin and V.V. Trachevskii, *J. Coord. Chem.*, **31** (1994) 147.
- [18] D. Borchardt and S. Wherland, *Inorg. Chem.*, **25** (1986) 901.
- [19] D. Borchardt, K. Pool and S. Wherland, *Inorg. Chem.*, **21** (1982) 93.
- [20] M.A. Murguia, D. Borchardt and S. Wherland, *Inorg. Chem.*, **29** (1990) 1982.
- [21] R. Epton, G. Mark and G.K. Rogers, *J. Organomet. Chem.*, **150** (1978) 93.
- [22] J.F. Coetzee (ed.), *Recommended Methods for Purification of Solvents and Tests for Impurities*, Pergamon Press, London, 1983.
- [23] M. Dietrich and J. Heinze, *J. Am. Chem. Soc.*, **112** (1990) 5142.
- [24] SHELXTL, *User Manual, Rev. 3*, Nicolet XRD Corp., Madison, WI, July 1981.
- [25] G.M. Bancroft, M.J. Hays and B.E. Pater, *J. Chem. Soc. A*, (1970) 956.
- [26] A.Yu. Nazarenko, E.V. Polshin and Ya.Z. Voloshin, *Mendeleev Commun.*, (1993) 45.
- [27] V.E. Zavodnik, V.K. Belsky, Ya.Z. Voloshin and O.A. Varzatsky, *J. Coord. Chem.*, **28** (1993) 97.
- [28] S.V. Lindeman, Y.T. Struchkov and Ya.Z. Voloshin, *Inorg. Chim. Acta*, **184** (1991) 107.
- [29] Ya.Z. Voloshin, S.V. Lindeman and Yu.T. Struchkov, *Koord. Khim.*, **16** (1990) 1367.
- [30] V.E. Zavodnik, V.K. Belsky and Ya.Z. Voloshin, *Polish J. Chem.*, **67** (1993) 1567.
- [31] S.V. Lindeman, Yu.T. Struchkov and Ya.Z. Voloshin, *J. Coord. Chem.*, **28** (1993) 319.
- [32] E. Larsen, G.N. La Mar, E.B. Wagner and R.H. Holm, *Inorg. Chem.*, **11** (1972) 2652.
- [33] A.B.P. Lever, *Inorganic Electronic Spectroscopy*, Elsevier, Amsterdam, 1984.
- [34] K. Nakamoto, *Infrared and Raman Spectra of Inorganic and Coordination Compounds*, Wiley, New York, 1986.